Alterations of auditory sensory gating in mice with noise-induced tinnitus treated with nicotine and cannabis extract

Barbara Ciralli[1], Thawann Malfatti[1,3], Thiago Z. Lima[1,2], Sérgio Ruschi B. Silva[1], Christopher R. Cederroth[3,4], Katarina E. Leao[1]*

[1]Brain Institute, Federal University of Rio Grande do Norte, Natal, RN, Brazil
[2]Department of Applied Mathematics and Statistics, Exact and Earth Sciences Center, Federal University of Rio Grande do Norte, Natal, RN, Brazil
[3]Experimental Audiology, Department of Physiology and Pharmacology, Karolinska Institutet, 171 77 Stockholm, Sweden
[4]Hearing Sciences, Division of Clinical Neuroscience, School of Medicine, University of Nottingham, NG7 2UH Nottingham, UK

*katarina.leao@neuro.ufrn.br
Brain Institute, Federal University of Rio Grande do Norte, Av. Senador Salgado Filho, 3.000, Campus Universitário Lagoa Nova, CEP 59078-970, postal box 1524, Natal-RN, Brazil

Abstract

Aims/Hypothesis: Tinnitus is a phantom sound perception affecting both auditory and limbic structures. The mechanisms of tinnitus remain unclear and it is debatable whether tinnitus alters attention to sound and the ability to inhibit repetitive sounds, a phenomenon also known as auditory gating.

Methods: 22 male C57BL/6J mice were used in this study. Anesthetized mice were exposed to a 9-11 kHz narrow band noise (90 dBSPL for 1 hr) and sham exposed mice were used as controls. Hearing thresholds were measured using auditory brainstem responses (ABRs) and tinnitus was assessed using Gap prepulse inhibition of acoustic startle (GPIAS). After the induction of tinnitus, mice were implanted multi-electrodes to assess auditory event-related potentials (aERPs) in the dorsal hippocampus in response to paired clicks. Alterations of aERPs under nicotine (1.0 mg/kg, intraperitoneal (i.p.) or cannabis extract (100 mg/Kg, i.p.) were evaluated (in isolation or in combination), the latter containing 47.25 mg/kg of tetrahydrocannabinol (THC); 0.43 mg/kg of cannabidiol (CBD) and 1.17 mg/kg of cannabinol (CBN), as analyzed by high-performance liquid chromatography (HPLC). Saline-treated animals were used as controls.

Results: Our results show that mice with behavioral evidence of tinnitus display auditory gating of repetitive click, but with larger amplitudes and longer latencies of the N40 component. In contrast, no difference was observed in the P80 amplitude and latency between groups or treatments. The combination of cannabis extract and nicotine also improved auditory gating ratio in mice with noise-induced tinnitus without permanent hearing threshold shifts by strongly increasing the first N40 click amplitude but without altering the second click response amplitude. Furthermore, the increased latency of the N40 component suggests altered temporal processing of triggered attention in mice with tinnitus due to an increased sensitivity to the exposure to cannabis extract.

Conclusion/Interpretation: In summary, we show that nicotine and cannabis extract alter sensory gating in mice with behavioral evidence of tinnitus and propose that the altered central plasticity in tinnitus is more sensitive to the combined actions on the cholinergic and the endocannabinoid systems. We conclude that the limbic system may play a role in the altered sensory gating responses on tinnitus since the hippocampus responses to auditory inputs are altered. These findings could enable a new understanding of which neuronal pathways could be involved in sensory gating in tinnitus.

Keywords: Tinnitus, Hippocampus, auditory event-related potentials, ABR, GPIAS, limbic

Introduction

Subjective tinnitus is a phantom sound sensation without an external source that is related to comorbidities such as anxiety and depression (Langguth et al., 2011) and decreased quality of life (Hiller and Goebel, 2006). Tinnitus affects around 15% of the world population (Biswas et al., 2022) and so far cognitive behavioral therapy is the only evidence-based recommended treatment (Cima et al., 2019). A relationship between tinnitus and decreased understanding of speech-in-noise has been reported (Tai and Husain, 2019) but it remains unclear whether chronic tinnitus directly interferes with speech-in-noise processing (Zeng et al., 2020), or whether this is a result of attentional problems that have been difficult to assess in tinnitus subjects (Tai and Husain, 2019). The limbic sys-

tem is implicated in the manifestation and development of chronic tinnitus (Chen et al., 2015), and PET and fMRI studies have shown greater activation of the auditory cortex, as well as non-auditory areas (frontal areas, limbic system and cerebellum) in tinnitus patients compared to controls (Lanting et al., 2009). Animal models of tinnitus point to neuronal alterations in the dorsal cochlear nucleus (Shore et al., 2016), affecting upstream auditory nuclei, with previous evidence of altered activity of the auditory cortex (Asokan et al., 2018). The auditory cortex has been shown to have significantly reduced functional connectivity with limbic structures (such as the hippocampus and amygdala) when comparing regional fMRI low-frequency activity fluctuations in a mouse model of noise-induced tinnitus (Qu et al., 2019). Still, the involvement of limbic structures in noise-induced tinnitus remains poorly investigated.

Processing of auditory input in limbic structures such as the hippocampus can be measured by event-related potential (ERP) for sensory gating, which is defined as a reduction in ERP to a repeated identical stimulus. Auditory sensory gating can be assessed with paired-click stimuli (0.5 s apart) where the auditory ERP (aERP) magnitude in response to the second click generates a smaller amplitude compared to the first. In humans, aERPs are measured using EEG, while in mice aERPs are often recorded using intra-hippocampal chronically implanted electrodes (Amann et al., 2008; Rudnick et al., 2010). An incomplete suppression of the second click represents abnormal sensory processing, and poor "gating" of paired auditory stimuli (Lijffijt et al., 2009). A decrease in sensory gating has been shown to be correlated with tinnitus severity in young adults (Campbell et al., 2018), whereas an increased latency in aERP was found in tinnitus patients (Santos Filha and Matas, 2010). Still, the neuronal correlates of aERPs are poorly understood and animal models of noise-induced tinnitus measuring auditory gating are largely lacking even though the aERP waveform of rodents, described as positive (P) or negative (N) peaks, with approximate latency in milliseconds, P20, N40 and P80 (Amann et al., 2008) or P1, N1 and P2, are analogous to the human waveforms (P50, N100 and P200).

Pharmacologically it has been shown that certain nicotinic acetylcholine receptors take part in augmenting auditory event-related potentials (Amann et al., 2008; Rudnick et al., 2010). Moreover, ERPs of subjects smoking cigarettes also containing different doses of cannabis have shown decreased ERP amplitude and to suffer acutely diminished attention and stimulus processing after smoking cannabis (Böcker et al., 2010). On the contrary, a combined activation of the cholinergic and the endocannabinoid system has shown to improve auditory deviant detection and mismatch negativity ERPs in human subjects, but not when each drug was delivered alone (Salle et al., 2019). This indicates interactions between the two systems, however, the impact of nicotine and/or cannabis, on auditory ERPs in animal models of tinnitus, has to our knowledge not yet been studied. Here, we first hypothesized that noise-induced tinnitus interferes with auditory gating, and next that nicotine or natural extracts of cannabis could improve auditory pre-attentional processing in noise-induced tinnitus. To test this, we used a mouse model of noise-induced tinnitus without hearing impairment and measured aERPs in the dorsal hippocampus in response to paired clicks.

Methods

Animals

C57BL/6J mice (1 month old at the beginning of the experimental timeline) originated from an in house-breeding colony. Since female C57BL/6J mice have significantly larger aERPs than male mice (Amann et al., 2008), only males were used in order to compare results with previous literature on sensory gating (Rudnick et al., 2010). Here we used a total of 29 mice, where 7 were excluded in GPIAS initial screening due to poor GPIAS (see exclusion criteria at the GPIAS section), leading to a total of 22 mice reported in all experimental procedures. Before the beginning of experiments, the animals were randomly assigned using python scripts (see section 2.11) to the Sham (n = 11) or Noise-induced tinnitus (n = 11) group. From those, 3 animals were excluded from ERP recordings due to low signal-to-noise ratio and 2 animals died after surgery (remaining 10 Sham and 7 Noise-induced tinnitus). Animals were housed on a 12/12h day/night cycle (onset/offset at 6h/18h) at 23ºC to maintain normal circadian rhythm and had free access to water and food pellets based on corn, wheat and soy (Nuvilab, Quimtia, Brazil;: #100110007, Batch: 0030112110). All experiments were performed during the day cycle, ranging from 7h to 15h. Animals (2-4 per cage) were housed in IVC cages, and paper and a polypropylene tube was added as enrichment. Once implanted, animals were single-housed until the end of the experiment. Mice were tunnel handled for the experiments as it has been shown to impact stress during experimental procedures, while tail-handling was used for routine husbandry procedures. All protocols were

approved by and followed the guidelines of the ethical committee of the Federal University of Rio Grande do Norte, Brazil (CEUA protocol no.094.018/2018).

Auditory brainstem responses

The sound equipment was calibrated in a sound-shielded room with an ultrasonic microphone (4939-A-011, Brüel and Kjær) for each of the stimuli used, with background noise of ≈35 decibel sound pressure level (dBSPL). The auditory brainstem response (ABR) of mice was tested both before and after the noise exposure protocol. Mice were anesthetized with an intraperitoneal injection (10 μl/gr) of a mixture of ketamine/xylazine (90/6 mg/kg) plus atropine (0.1 mg/kg) and placed in a stereotaxic apparatus on top of a thermal pad with a heater controller set to 37°C and ear bars holding in front of and slightly above the ears, on the temporal bone, to not block the ear canals. The head of the animal was positioned 11 cm in front of a speaker (Super tweeter ST400 trio, Selenium Pro). To record the ABR signal, two chlorinated electrodes were used, one recording electrode and one reference (impedance 1 kΩ) placed subdermally into small incisions in the skin covering the bregma region (reference) and lambda region (recording). Sound stimulus consisted of narrow-band gaussian white noise pulses with length of 3 ms each, presented at 10 Hz for 529 repetitions at each frequency and intensity tested. The frequency bands tested were: 8-10 kHz, 9-11 kHz, 10-12 kHz, 12-14 kHz and 14-16 kHz. Pulses were presented at 80 dBSPL in decreasing steps of 5 dBSPL to the final intensity 45 dBSPL as previously described (Malfatti et al., 2022). The experimenter was blinded to the animal group during the ABR recordings.

Gap prepulse inhibition of acoustic startle (GPIAS)

The Gap prepulse inhibition of acoustic startle (GPIAS) test (Turner et al., 2006), was used to infer tinnitus in noise-exposed mice. GPIAS evaluates the degree of inhibition of the auditory startle reflex by a short preceding silent gap embedded in a carrier background noise. Mice were initially screened 3 days before the noise exposure for their ability to detect the gap. Animals were then tested again 3 days after noise exposure or sham procedures (no noise), as previously described (Malfatti et al., 2022). In detail, animals were placed in custom-made acrylic cylinders perforated at regular intervals. The cylinders were placed in a sound-shielded custom-made cabinet (44 x 33 x 24 cm) with low-intensity LED lights in a sound-shielded room with ≈35 dBSPL (Z-weighted) of background noise. A single loudspeaker (Super tweeter ST400 trio, Selenium Pro, freq. response 4-18 kHz) was placed horizontally 4.5 cm in front of the cylinder, and startle responses were recorded using a digital accelerometer (MMA8452Q, NXP Semiconductors, Netherlands) mounted to the base plate of the cylinder and connected to an Arduino Uno microcontroller, and a data acquisition cart (Open-ephys board) analog input. Sound stimuli consisted of 60 dBSPL narrow-band filtered white noise (carrier noise); 40 ms of a silent gap (GapStartle trials); 100 ms of interstimulus interval carrier noise; and 50 ms of the same noise at 105 dBSPL (startle pulse), with 0.2ms of rise and fall time. The duration of the carrier noise between each trial (inter-trial interval) was pseudo-randomized between 12-22 s. Test frequencies between 8-10, 9-11, 10-12, 12-14, 14-16 and 8-18 kHz were generated using a butterworth bandpass filter of 3rd order. The full session consisted of a total of 18 trials per frequency band tested (9 Startle and 9 GapStartle trials per frequency, pseudo-randomly played). It was previously shown that mice can suppress at least 30% of the startle response when the loud pulse is preceded by a silent gap in background noise (Li et al., 2013), therefore we retested frequencies to which an animal did not suppress the startle by at least 30% in a second session the next day. Animals that still failed to suppress the startle following the silent gap in at least two frequencies in the initial GPIAS screening were excluded from further experiments. The experimenter was blinded to the animal group during the GPIAS recordings.

Noise exposure

Mice were anesthetized with an intraperitoneal administration of ketamine/xylazine (90/6 mg/kg), placed inside an acrylic cylinder (4 x 8 cm) facing a speaker (4 cm distance) inside a sound-shielded cabinet (44 x 33 x 24 cm) and exposed to a narrow-band white noise filtered (butterworth, -47.69dBSPL/Octave) from 9-11 kHz, at an intensity of 90 dBSPL for 1 hr, and next remained in the cylinder inside the sound shielded chamber for 2 hours, as sound-enrichment post loud noise exposure may prevent tinnitus induction (Sturm et al., 2017). Sham animals were treated equally, but without any sound stimulation. The animals were then returned to their home cages.

Electrode array assembly

Tungsten insulated wires of 35 μm diameter (impedance 100-400 kΩ, California Wires Company) were used to manufacture 2 x 8 arrays of 16 tungsten wire electrodes. The

wires were assembled to a 16-channel custom made printed circuit board and fitted with an Omnetics connector (NPD-18-VV-GS). Electrode wires were spaced by 200 μm with increasing length distributed diagonally in order to record from different hippocampal layers, such that, after implantation, the shortest wire were at dorsoventral (DV) depth of -1.50 mm and the longest at DV -1.96 mm. The electrodes were dipped in fluorescent dye (1,1'-dioctadecyl-3,3,3',3'-tetramethylindocarbocyanine perchlorate; DiI, Invitrogen) for 10 min (for post hoc electrode position) before implanted into the right hemisphere hippocampus.

Electrode array implantation

22 animals were used for the electrodes implantation surgery. In detail, mice were anesthetized using a mixture of ketamine/xylazine (90/6 mg/kg) and placed in a stereotaxic frame on top of a heat pad (37°C). Dexpanthenol was applied to cover the eyes to prevent ocular dryness. When necessary, a bolus of ketamine (45 mg/kg) was applied during surgery to maintain adequate anesthesia. Iodopovidone 10% was applied on the scalp to prevent infection, and 3% lidocaine hydrochloride was injected subdermally before an incision was made. In order to expose the cranial sutures, 3% hydrogen peroxide was applied over the skull. Four small craniotomies were done in a square at coordinates mediolateral (ML) 1 mm and anteroposterior (AP) -2.4 mm; ML: 1 mm and AP: -2.6 mm; ML: 2.45 mm and AP: -2.4 mm; ML: 2.45 mm and AP: -2.6 mm, to make a cranial window were the electrodes were slowly inserted at DV coordinate of -1.9 mm (for the longest shank). Four additional holes were drilled for the placement of anchoring screws, where the screw placed over the cerebellum served as reference. The electrode implant was fixed to the skull with polymethyl methacrylate moldable acrylic polymer around the anchor screws. After surgery, the animals were monitored until awake and then housed individually and allowed to recover for one week before recordings. For analgesia, ibuprofen 0.04 mg/ml was administered in the water bottle 2 days before and 3 days after the surgery. Subcutaneous Meloxicam 5 mg/kg was administered for 3 consecutive days after the surgery. 2 animals died shortly after the surgery, remaining 10 animals in the sham group and 7 in the noise-induced tinnitus group.

Paired-click stimuli for auditory event related potentials

Mice were habituated during two days in the experimental setup and in the day of recording, anesthesia was briefly induced with isoflurane (5% for <1 min) to gently connect the implanted electrode array to a head-stage (intan RHD 2132) connected to an acquisition board (OpenEphys v2.2 XEM6010-LX150) by a thin flexible wire. Auditory event-related potentials (aERPs) were recorded in freely moving animals placed in a low-light environment exposed to paired click stimulus, played by a speaker (Selenium Trio ST400) located 40 cm above the test area. All recordings were performed in standard polycarbonate cage bottom, which was placed inside a sound-shielded box (40 x 45 x 40 cm). The paired clicks consisted of white noise filtered at 5-15 kHz presented at 85 dBSPL, 10 ms of duration, and 0.5 s interstimulus interval. Stimulus pairs were separated by 2-8 s (pseudorandomly), and a total of 50 paired stimuli were presented. The session duration varied from 148 s to 442 s.

To in detail investigate auditory ERPs, average data from different animals, and also, compare responses from different experimental days and different pharmacological treatments, the appropriate hippocampal location for picking up aERP was identified. As local field potentials are related to cell density, and thereby the resistivity of the tissue, it is useful to record from the hippocampus with its distinct layered structure that shows phase-reversals of local field potentials (Scheffer-Teixeira et al., 2012). Responses to paired clicks were recorded one week after surgery. The grand average of aERP (average of 50 clicks) for each channel was plotted and the changed signal polarity across hippocampal layers was identified, as the electrode array channels were distributed at different depths (Figure 3A-B). To facilitate comparison of aERP between implanted animals we selected the first channel above phase reversal (Figure 3B, gray dashed rectangle) that showed a clear negative peak followed by a positive peak in the deeper channel. The visualization of the phase reversal channel was routinely added to analysis as channels sometimes shifted in the same animal, likely due to small movements in the electrode array when connecting/disconnecting mice to/from the headstage during different recording sessions. The experimenter was blind to the animal group during the ERP recordings.

Cannabis sativa extract production and analysis

Here we used a cannabis extract instead of pure agonists, which is more representative of the human exposure than the use of pure THC or other synthetic agonists (Wilkinson et al., 2003; Salle et al., 2019). THC is the main psychoactive compound in cannabis and it is known to

be partial agonist of CB1 and CB2 receptors (Sampson, 2020), while CBN activates CB1 and CB2 receptors with more affinity over the latter and CBD acts as a negative allosteric modulator of CB1 (Sampson, 2020). The Cannabis sativa extract was produced from an ethanolic extraction with the flowers previously dried and crushed. After leaving them in contact with the solvent for 5 min in an ultrasonic bath, filtration was performed and the process was repeated twice. Additionally, the solvent was evaporated and recovered, leaving only the cannabis extract in resin form. Decarboxylation of the acidic components, mainly tetrahydrocannabinolic acid (THCA) into delta-9-tetrahydrocannabinol (THC), was carried out by heating the material at 90°C until the conversion to the neutral forms had been completed. The cannabis extract was analyzed by high-performance liquid chromatography (HPLC). Analytical standards of THC (Cerilliant T-005), cannabinol (CBN, Cerilliant C-046) and cannabidiol (CBD, Cerilliant C-045) were used in the calibration curve dilutions. An Agilent 1260 LC system (Agilent Technologies, Mississauga, ON, Canada) was used for the chromatographic analysis. A Poroshell 120 EC-C18 column (50 mm × 3.0 mm, 2.7 μm, Agilent Technologies) was employed, with a mobile phase at a flow rate of 0.5 mL/min and temperature at 50°C (separation and detection). The compositions were (A) water and (B) methanol. 0.1% formic acid was added to both water and methanol. The total analysis time was 18 min with the following gradient: 0–10 min, 60–85%B; 10–11 min, 85–100%B; 11-12 min, 100%; 12-17 min, 100–60%; 17-18 min, 60% the temperature was maintained at 50°C (separation and detection). The injection volume was 5 μL and the components were quantified based on peak areas at 230 nm. During the experiments we used a single dose of cannabis extract for each animal (100 mg/Kg), containing 47.25 mg/kg of tetrahydrocannabinol (THC); 0.43 mg/kg of cannabidiol (CBD) and 1.17 mg/kg of cannabinol (CBN) as analyzed by high-performance liquid chromatography (HPLC), and kindly donated by the Queiroz lab, Brain Institute, Federal University of Rio Grande do Norte, Brazil.

Pharmacology

To activate the cholinergic system, and specifically brain nicotinic acetylcholine receptors, animals received a single intraperitoneal injection of nicotine (Sigma N3876) at 1.0 mg/kg (Metzger et al., 2007) or saline (randomized order, 2 days in between session 1 and 2) 5 minutes before aERP recordings. Since THC, CBD and CBN have a longer half-life, approximately 110 min in mouse plasma (Torrens et al., 2020), 3.9h in mouse plasma (Xu et al., 2019) and 32h in human plasma (Johansson et al., 1987) respectively, when compared to nicotine (approximately 6-7 min (Petersen et al., 1984)), we treated with cannabis last (3rd session) at a single dose of cannabis extract (100 mg/Kg). On the experimental day, the cannabis extract resin was diluted in corn oil to 10 mg/ml solution by mixing the extract and the oil and then sonicating for 5 min before injected intraperitoneally (at volume of 10 μl/gr body weight) 30 min prior to aERP recording sessions to reach max plasma concentration of THC (Torrens et al., 2020). After the third recording session, an additional dose of nicotine (1 mg/Kg) was injected (to study potentially synergistic effects of cannabis extract + nicotine) and the animals were recorded 5 min later to observe how the interaction of the cholinergic and endocannabinoid system affects aERPs. After each aERP recording session, mice were unconnected from the headstage and returned to their home cage.

Histology

To verify expected electrode positioning, animals were deeply anesthetized at the end of the experimental timeline with a mixture of ketamine/xylazine (180/12 mg/kg) and transcardiac perfused with cold phosphate buffered saline (PBS) followed by 4% paraformaldehyde (PFA). Brains were dissected and placed in 4% PFA for 48 hrs. Next, brains were sliced using a free-floating vibratome (Leica VT1000S) at 75 μm thickness, and cell nuclei were stained with 4',6-diamidino-2- Phenylindole (DAPI, Sigma) to visualize cell layers and borders of the hippocampus. In addition to DiI-staining the electrodes, a current pulse of 500 μA was routinely passed through the deepest electrode for 5 s at the end the last aERP recordings to cause a small lesion around the electrode tip to confirm electrode depth. Images were visualized using a Zeiss imager A2 fluorescence microscope with a N-Achroplan 5x objective.

Data Analysis

Analysis of auditory brainstem responses was done as previously described (Malfatti et al., 2022) and consisted of averaging the 529 trials, filter the signal using a 3rd order butterworth bandpass filter from 600-1500 Hz, and slice the data 12 ms after the sound pulse onset. Thresholds were defined by automatically detecting the lowest intensity that can elicit a wave peak one standard deviation above the mean, and preceded by a peak in the previous intensity (Malfatti et al., 2022). Effect of noise exposure

on ABR thresholds was evaluated using the Friedman Test, and pairwise comparisons were performed using the Wilcoxon test. Effect of noise exposure on ABR threshold differences before and after exposure was evaluated using two-way ANOVA (Group x Frequency of stimulus as factors). When multiple comparisons within the same dataset were performed, p values were Bonferroni-corrected accordingly.

For each frequency tested in GPIAS, Startle and GapStarle trials responses were separated and the signal was filtered with a Butterworth lowpass filter at 100 Hz. The absolute values of the accelerometer axes, from the accelerometer fitted below the cylinders enclosing the mice during the modified acoustic startle test, were averaged and sliced 400 ms around the startle pulse (200 ms before and 200 ms after). The root-mean-square (RMS) of the sliced signal before the Startle (baseline) was subtracted from the RMS after the startle response (for both Startle only and GapStartle sessions). The GPIAS index for each frequency was then calculated as

$$\left(1 - \left(\frac{GapStartleRMS}{StartleRMS}\right)\right) * 100$$

generating percentage of suppression of startle. For each animal, the most affected frequency was determined as the frequency with the greatest difference in GPIAS index before and after noise exposure. This was done as mice did not show decreased GPIAS at the same narrow-band frequency despite being subjected to the same noise exposure, indicating individual differences in possible tinnitus perception (Longenecker and Galazyuk, 2016). The definition of the most affected frequency followed the same procedure for both sham and noise-induced tinnitus animals. The effects of group (sham or noise-exposed), epoch (before or after exposure) and frequency of stimulus were tested using 3-way mixed models ANOVA. The effect of the noise exposure on the GPIAS index of the most affected frequency was evaluated using the Friedman test, and pairwise comparisons were done using the Wilcoxon test.

Auditory event-related potentials in response to paired-clicks were filtered using a low pass filter at 60 Hz, sliced 0.2 s before and 1 s after the first sound click onset, and all 50 trials were averaged. To compare signals between different animals (n=10 sham and n=7 noise-induced tinnitus) and different treatments we always analyzed the channel above hippocampal phase reversal with a negative peak around 40 ms (N40) and a positive peak around 80 ms latency (P80). Auditory ERP components were quantified by peak amplitude (baseline-to-peak) after stimulus onset. The N40 was considered as the maximum negative deflection between 20 and 50 ms after the click stimulus, and P80 as the maximum positive deflection after the N40 peak. The baseline was determined by averaging all 50 trials and then averaging the 200 ms of prestimulus activity (before the first click). The latency of a component was defined as the time of occurrence of the peak after stimulus onset. The ratio in percentage of the first and second click amplitude (the suppression of the second click, e.g. sensory filtering) was calculated as

$$\left(1 - \left(\frac{SecondClickAmplitude - Baseline}{FirstClickAmplitude - Baseline}\right)\right) * 100$$

and error bars represent standard error of the mean (s.e.m) for all figures. Nonparametric ANOVA was used to test pointwise measurement of amplitude and latency at N40 and P80, whenever the response failed to comply with normality, homoscedasticity and independence assumptions and parametric fitting was inadequate. Under the nonparametric framework, post-hoc multiple comparisons were adjusted by Bonferroni correction. Differences in ERPs N40-P80 peak width were evaluated using mixed-models ANOVA, and differences in occurrence of double-peak responses were evaluated using McNemar's test.

Functional data analysis of auditory event-related potentials

Statistical analysis used for functional data analysis (Figure S6) was carried out with R software and the functional data analysis package (see Data and Code Availability Statement). In brief, local field potentials (LFP) in the channel above phase reversal from sham and noise-induced tinnitus mice (n = 6 per group, data from first cohort with adequate signal-to-noise ratio) were downsampled to 600Hz with frequencies > 60 Hz filtered out. A time window of 200 ms before and 1 s after the first sound click was used for analysis. The LFP from each trial was individually fitted into a function corresponding to a linear combination of a Fourier expansion with a 121-basis function, whose coefficients were determined by least squares regression. Further smoothing was achieved as the mean function was computed from the repetitions from each animal at each experimental condition, and mean functions were used in further analysis. Next, a functional principal component analysis (FPCA) was carried out to explore the main patterns of variability in the data. The VARIMAX algorithm for rotation was used to improve interpretation of the principal components. In addition to providing visual clusterization of the data, principal

components were also used as the variables for inferential tests of the significance of the effects from experimental factors (Condition; noise-induced tinnitus and sham animals and Treatment; saline, nicotine, cannabis extract and cannabis extract plus nicotine). Since the experiment was done in a two-factor design with repeated measures in only one, principal components were tested by means of (mixed) repeated measures ANOVA with Condition as between (or whole plot) factor and Treatment as within (or subplot) factor (and animals or replicates as a random factor). The validity of the test was checked by residual analysis and Tukey's procedure for multiple comparison was carried out as a post-hoc test to describe the effect of treatment, whenever it had been identified as statistically significant by ANOVA. A 95% joint confidence level was considered for multiple comparisons.

Results

We first aimed to reproduce a model of noise-induced tinnitus with a normal audiogram, as reported in both humans and animals (Longenecker and Galazyuk, 2016; Campbell et al., 2018; Qu et al., 2019). In order to investigate whether noise-exposure can affect auditory gating we established an experimental timeline for experiments evaluating auditory perception using three different tests: Auditory brainstem responses (ABRs), Gap prepulse inhibition of acoustic startle (GPIAS) and Auditory event-related potentials (aERPs). Hearing thresholds of mice were assessed using ABRs 2 days before (baseline) and 2 days after sham or noise exposure (Figure 1A). ABRs showed field potentials with distinct peaks indicating neuronal activity at the auditory nerve, cochlear nuclei, superior olivary complex, and inferior colliculus (Henry, 1979) in response to sound clicks presented at different frequencies (Figure 1B-C). Similar to sham, noise exposure did not cause any change in ABR hearing thresholds at all frequencies tested when compared to baseline (Friedman eff. size <0.58, $p > 0.08$; Figure 1D). Threshold shifts confirmed that noise-exposed animals were impacted to a similar degree than sham mice ($F(4,84) < 2.021$, $p > 0.09$; Figure 1E). Unlike other models of tinnitus (Zhang et al., 2020), we did not detect any difference in ABR Wave 1 amplitude (Kruskal-Wallis, eff. size < 0.012, $p > 0.14$) or Wave 5 latency (Kruskal-Wallis, eff.size < 0.011, $p > 0.073$, Figure S1). These findings confirm that the noise exposure did not cause any detectable change in hearing thresholds.

Three days before and 3 days after noise exposure mice were tested for GPIAS (Figure 2A-C). No effect of group (sham or noise-induced tinnitus), epoch (before or after noise exposure procedure) or frequency of stimulus was found in GPIAS when evaluating all frequencies from every animal ($F(5,65) < 1.419$, $p > 0.229$; Figure 2D-E), possibly due to each individual mouse may experience a different tinnitus pitch. We therefore evaluated the background frequency that interferes most with gap prepulse startle suppression for each individual mouse, which would correspond to the most likely tinnitus pitch of these animals (Figure 2F-G). Sham exposure had no effect on GPIAS (Friedman test; eff.size = 0.075; p = 0.365; Figure 2F, left), while in noise-induced tinnitus mice the noise exposure had a significant effect in GPIAS index (Friedman test; eff. size = 1.0; p = 1.8e-03), showing a decrease in startle suppression when comparing before and after noise exposure (Wilcoxon test, p=9.8e-04; Figure 2F, right). GPIAS showed individual variability (Figure 2G) similar to previously shown for noise-induced tinnitus in mice (Longenecker and Galazyuk, 2016) and confirms that tinnitus interferes with the ability to suppress the startle response in noise-induced tinnitus animals.

After the ABR and GPIAS tests, electrodes were implanted in the dorsal hippocampus for the assessment of sensory gating (Figure 3A). As expected, auditory event-related potential recordings showed that the second click consistently generated a smaller aERP (Figure 3B) and the magnitude of peaks around 40ms and 80ms were quantified from baseline as the N40 and P80 peak, respectively, for both the first and second click in the phase-reversal channel (see Methods, Figure 3B-C). Next, to investigate the impact of noise-induced tinnitus on auditory gating (11 days after noise-exposure), freely exploring mice were individually subjected to randomized paired-click stimuli where both sham and noise-induced tinnitus mice presented characteristic aERP (Figure 3D). Two types of measurements were evaluated: the responses to sound clicks measured in the hippocampus (amplitude in μV and latency in ms), which is a measurement of sound processing in the limbic system; and the ratio between the second and the first click responses (both amplitude and latency unitless), which measures the sensory gating.

As attention is modulated by the cholinergic system (Ballinger et al., 2016) and also the endocannabinoid system (Verrico et al., 2004), we tested the impact of two agonists to both systems (nicotine and cannabis extract, individually or in combination) in modulation of auditory ERPs in our model of noise-induced tinnitus (Figure 4A). The average of the N40 response in sham-exposed animals showed the second click to be consistently smaller in amplitude compared to the first click ($F(1,10) = 29.9$, $p =$

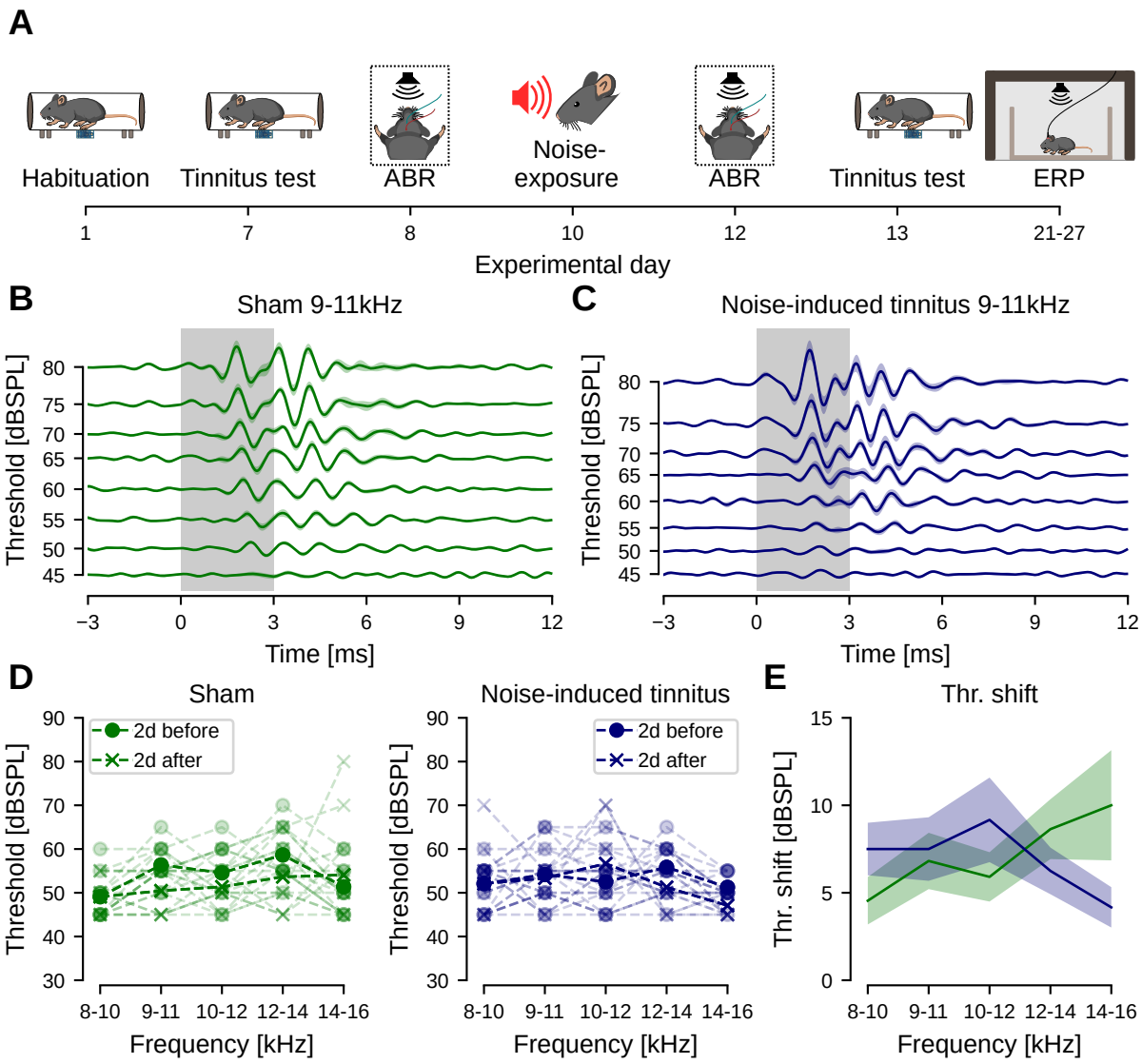

Figure 1: Noise exposure does not cause hearing threshold shift. A) Full experimental timeline highlighting time of ABR recordings (dotted rectangle). B-C) Mean auditory brainstem response (ABR) to 9-11kHz after noise-exposure for intensities 45-80 dBSPL for sham mice (B) and noise-induced tinnitus animals (C). Shaded traces show SEM, gray square indicates the sound pulse duration. D) Auditory thresholds quantified for sham (n = 11, left) and noise-induced tinnitus (n = 11, right) animals two days before and two days after noise exposure, showing no significant difference at any frequency tested (Wilcoxon test, $p > 0.05$ for all frequencies in both groups). E) Threshold shift for sham and noise-induced tinnitus mice showing no significant difference between groups (Student's t-test, $p > 0.05$ for all frequencies).

2.7e-04; Figure S2A, left). This significant attenuation on the second click was also observed for noise-induced tinnitus ($F(1,10) = 11.2$, $p = 7e\text{-}03$; Figure S2A, right). The second click attenuation differed in strength depending on the pharmacological treatment between sham and noise-induced tinnitus mice ($F(3,60) = 3.67$, $p = 1.7e\text{-}02$; Figure S2A). For noise-induced tinnitus animals the second click was smaller than the first in nicotine ($p = 1.6e\text{-}02$) and cannabis extract + nicotine ($p = 1.6e\text{-}02$) treatment but not in saline ($p = 0.237$) or cannabis extract alone ($p = 0.216$; Figure S2A, right), in contrast to sham animals. We therby found a significant interaction between treatment and animal condition (sham or noise-induced tinnitus) on the N40 suppression ratio ($F(3,60) = 3.5$, $p = 2e\text{-}02$, Figure 4B). Looking specifically at sham mice, no significant difference was found in the N40 aERP ratio between treatments, while for noise-induced tinnitus animals, pairwise comparisons showed an increased N40 amplitude ratio after administration of cannabis extract + nicotine compared to cannabis extract alone ($p = 1.9e\text{-}02$), nicotine alone ($p = 3.2e\text{-}02$) and NaCl treatment ($p = 1.9e\text{-}02$, Figure 4B). There was also a significant difference in N40 ratio under cannabis extract + nicotine treatment between sham and noise-induced tinnitus mice

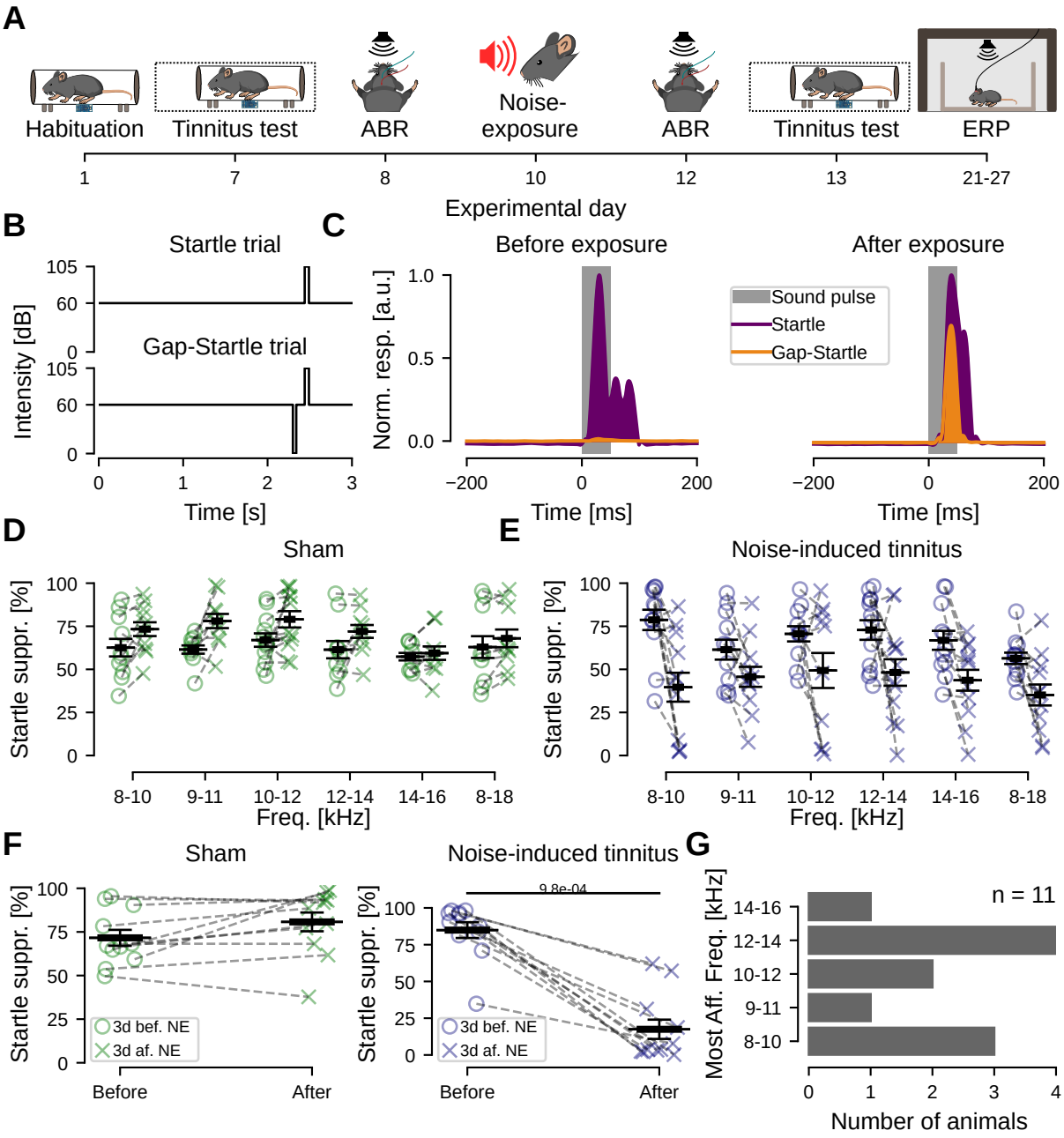

Figure 2: Noise-exposed animals showed decreased startle suppression. A) Timeline of experiments highlighting time point of the GPIAS tests. B) Schematic GPIAS protocol. C) Representative examples of startle suppression by the gap (left) and negative startle suppression (right) from the same animal 3 days before and 3 days after noise exposure, respectively. Filled traces represent an average of 9 trials of stimulus without gap (purple) and with gap (orange). Gray rectangle represents the 50ms startle stimulus. D-E) GPIAS index for all frequencies tested 3 days before (o) and 3 days after (x) noise exposure for sham (D) and noise-induced tinnitus (E) mice. F) The frequency with largest difference in startle suppression before and after noise-exposure was used for quantification of group GPIAS performance. Sham animals show no difference in GPIAS performance before and after noise exposure(left, n=11), while noise-induced tinnitus mice (right) show a significant decrease in startle suppression by the silent gap (Wilcoxon test, n = 11, p = 9.8e-04). G) The frequency with largest difference in startle suppression before and after noise-exposure varied between individual noise-induced tinnitus mice.

(p = 1.0e-02; Figure 4B). We found an overall effect of group (including all treatments and both clicks) in the N40 amplitude, where noise-induced tinnitus animals showed a greater average when compared to sham-exposed mice (sham-exposed amplitude: 156.3±8.7μV; noise-induced tinnitus amplitude: 220.7±17.4μV, p = 6.3e-03; Kruskal-Wallis; Figure 4C, Figure S2A). Taken together, these results indicate that nicotine has a more pronounced effect on the filtering of repetitive stimuli in noise-induced tinnitus animals compared to sham animals, and that

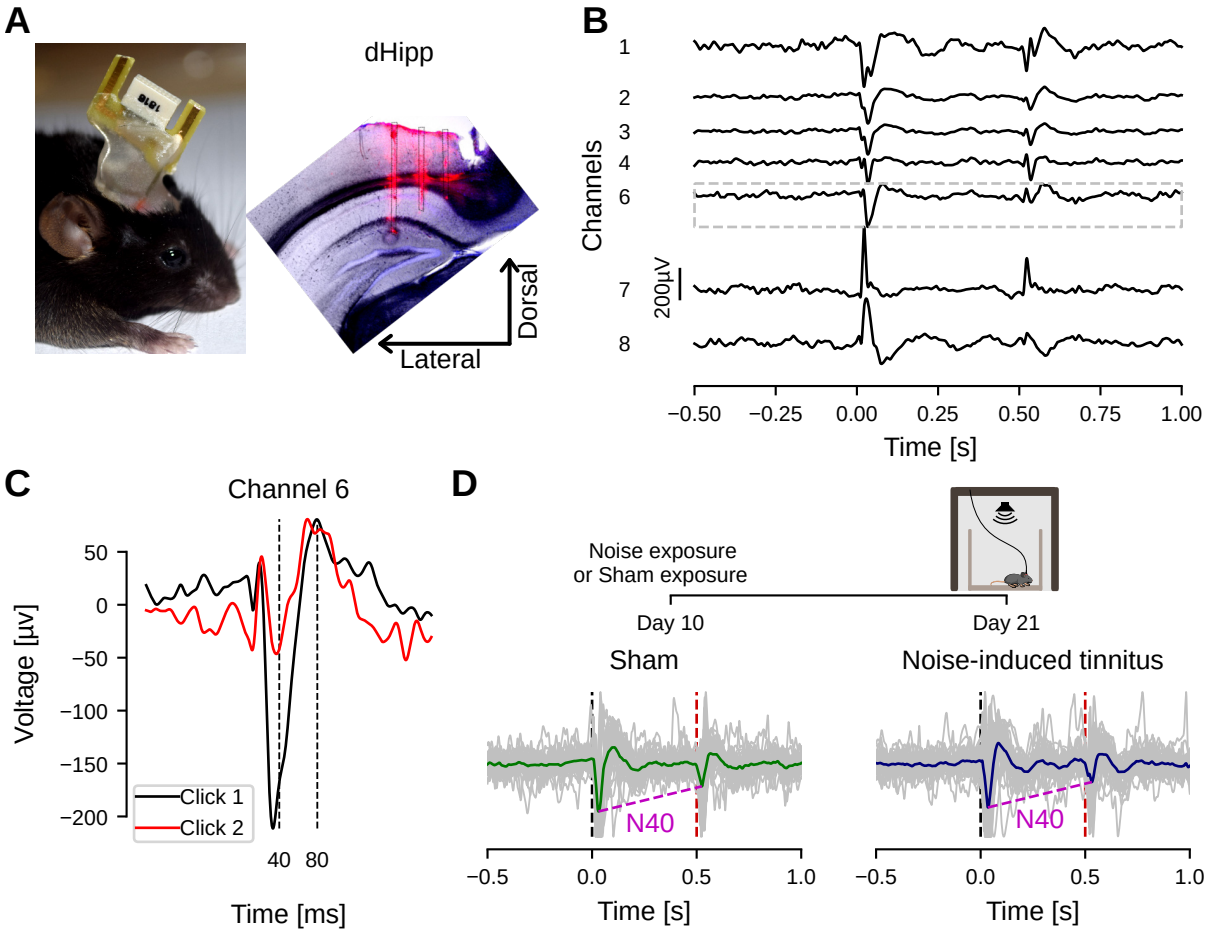

Figure 3: Auditory event-related potentials in sham and noise-induced tinnitus mice. A) Left, image of a mouse implanted with an electrode array. Right, coronal slice showing the dorsal hippocampus with electrode tracts stained with DiI in the CA1 region. B) Average aERPs in response to paired clicks from 8 channels at different depths from a recording session from a single animal. The channel above phase reversal (gray dotted box) was consistently used for aERP quantification. C) The reversal channel from 'B' at a greater magnification with click 1 (black) and 2 (red) responses superimposed. Dashed lines indicating positive and negative peaks at different characteristic latencies (N40 and P80 components). D) Top, simplified experimental timeline. Bottom, average traces of click responses in saline condition for sham (green, n = 10) and noise-induced tinnitus animals (blue, n = 7). Superimposed gray traces are the average response of 50 trials from each individual animal, dashed lines indicate the sound stimuli onset and amplitude difference of N40 peaks.

the combination of nicotine + cannabis extract strongly enhances the first and second click ratio in noise-induced tinnitus animals, an effect not seen in sham animals.

Examining latency of the N40 component showed no differences in pairwise comparisons between clicks after any particular treatment ($p>0.05$; Figure S2B) although the distribution of latencies showed the second N40 latency to be consistently shorter compared to the first (ANOVA-type statistic = 9.0449, DF = 1, p = 2.6e-03). Comparing the ratio of the first and second click latency revealed an increased response-delay in noise-induced tinnitus animals under cannabis treatment compared to sham animals in the same treatment (p = 3.0e-03) and compared to noise-induced tinnitus mice after nicotine administration (p = 3.2e-02; Figure 4D). This shows that cannabis delays the N40 latency compared to nicotine in noise-induced tinnitus animals but not in sham animals (Figure 4D). Overall, an effect of group on latency (including all treatments and both clicks) was found, where latency was increased for noise-induced tinnitus mice (sham-exposed latency: 29.9±0.9 ms, noise-induced tinnitus latency: 32.9±0.9 ms, p = 4.3e-02, Kruskal-Wallis; Figure 4E).

The P80 component of auditory ERP has been implicated in the NMDA dysfunction theory in schizophrenia, as ketamine can alter the P80 amplitude of mice (Connolly et al., 2004). The P80 component in response to the second click was consistently smaller compared to the response to the first stimulus ($F(1,20) = 6.156$, p = 2.2e-02). Also, the latency for the peak was reduced by the repetition of stimuli for both groups and all treatments ($F(1,20) = 9.79$, p = 5.2e-03). However, pairwise comparisons did not show any statistical differences for

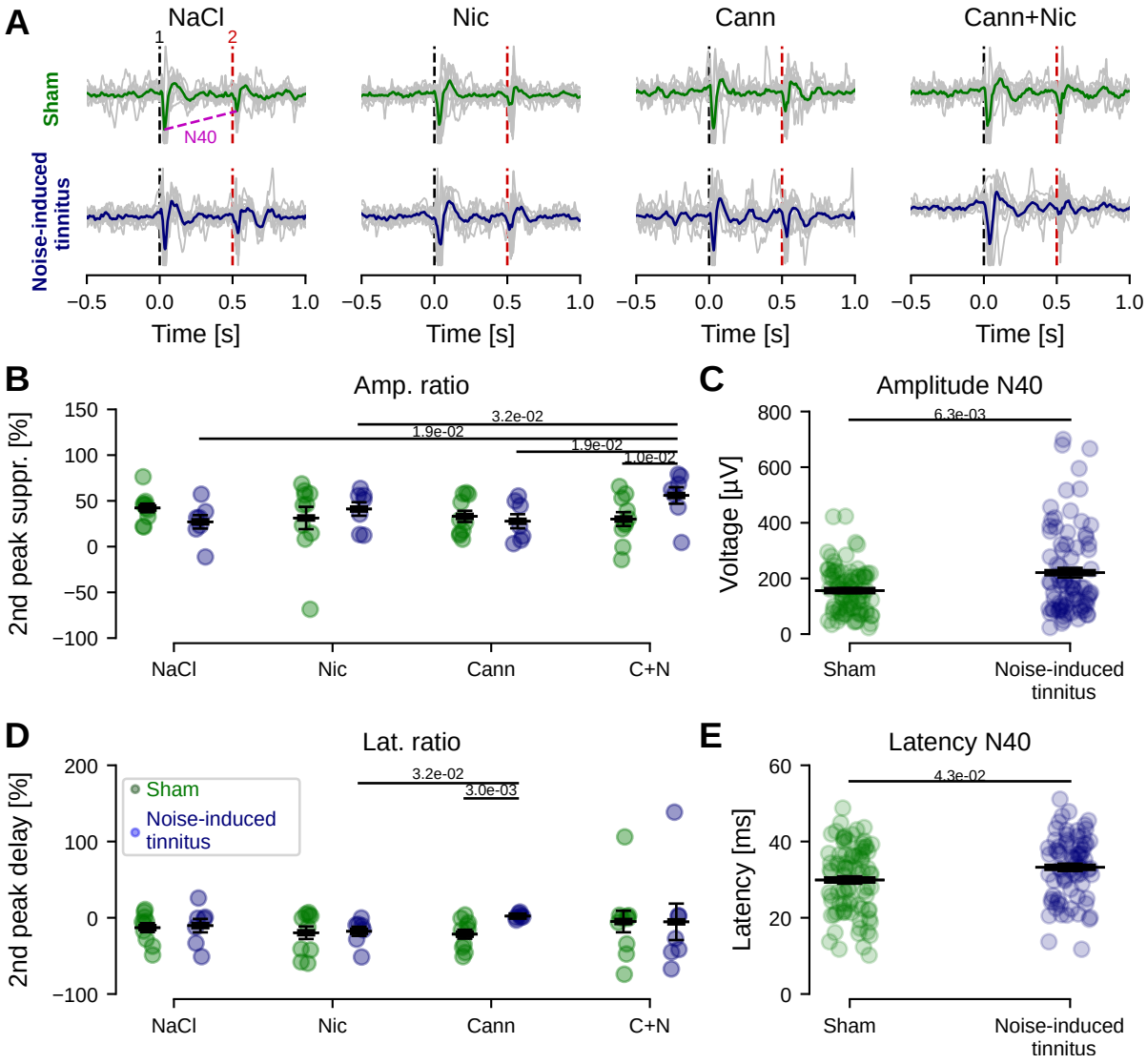

Figure 4: Auditory ERPs are larger and slower in noise-induced tinnitus mice after cannabis+nicotine treatment compared to sham mice. A) Auditory ERP recorded in awake mice in response to saline, nicotine, cannabis and cannabis+nicotine show characteristic suppression of the second click in both sham (top) and noise-exposed tinnitus (bottom) animals. Gray trace shows the average aERP per animal while the green and blue traces show the group average for each treatment. B) Percentage of suppression of the second click of the N40 component (supplementary Figure S2) for sham (green) and noise-induced tinnitus (blue) mice, showing largest suppression of the second peak in noise-induced tinnitus mice following cannabis+nicotine administration (Wilcoxon test). C) Group average of the N40 amplitude of sham (n = 10) and noise-induced tinnitus animals (n = 7) for both click 1 and click 2 for all pharmacological treatments (Kruskal-Wallis test). D) Percentage of the second N40 peak delay for both groups at each treatment showed cannabis extract to increase delay in noise-induced tinnitus mice compared to sham, as well as compared to nicotine treatment of noise-induced tinnitus mice (Wilcoxon test). E) Group average N40 latency for sham (n = 10) and noise-induced tinnitus animals (n = 7) for both click 1 and click 2 for all pharmacological treatments (Kruskal-Wallis test).

the P80 baseline to peak amplitude or latency (Figure 5A; Figure S3) nor in ratios between the two clicks for the P80 amplitude (Figure 5B) and latency (Figure 5D). This indicates that the P80 component is not affected by noise-induced tinnitus.

As previous studies suggested that the improvement of sensory gating by pharmacological agents is mediated by an enhancement of the first click rather than by the suppression of the second click (Amann et al., 2008; Rudnick et al., 2010), we separated the analysis of aERPs to focus on each click response (first; click 1 and repeated; click 2) by comparing the amplitude and latency of the N40 or P80 components between different treatments (Figure 6; Figure S4). First, we found that sham animals increase the response to the first click after cannabis extract + nicotine treatment compared to just nicotine administration (p = 4e-03; Figure 6A, top left). For the noise-induced tinnitus group, the combination of cannabis extract + nicotine increased click 1 amplitude compared to NaCl (p=1.2e-02; Figure 6A, top right). In noise-induced tinnitus mice

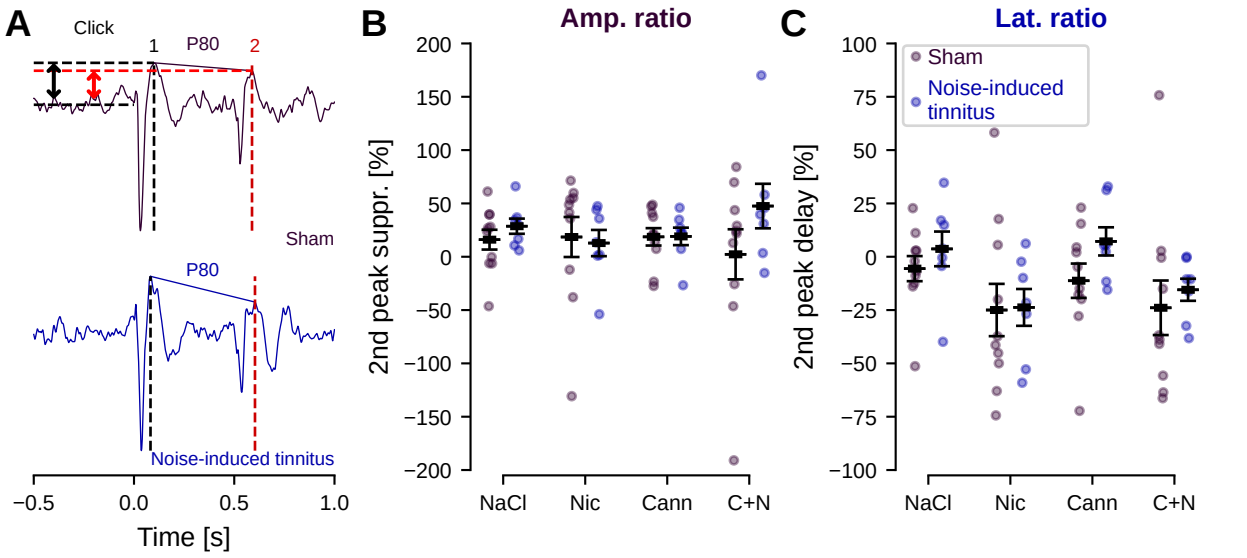

Figure 5: The P80 aERP amplitude and latency was not affected by noise-exposure or by nicotine and/or cannabis extract treatment. A) Representative trace highlighting the P80 component (vertical black and red dashed lines for first and second clicks, respectively). Arrows represent the calculated amplitude for each P80 response for the top trace. B) The percentage of second peak amplitude suppression showed no difference between sham and noise-induced tinnitus mice. C) Second P80 peak delay (ratio of the 1st and 2nd click responses latencies) for sham (purple) and noise-induced tinnitus (blue) animals showed no difference between groups or treatments. A negative 'delay' refers to a peak advancement. Wilcoxon test, n = 10 sham and 7 noise-induced tinnitus mice, $p > 0.05$ for all comparisons.

there was no increase in click 1 response by nicotine, but still nicotine had an effect in the combination of cannabis extract since the combination of the two increased the response amplitude significantly compared to cannabis extract alone (p = 4.7e-02; Figure 6A, top right). Next, examining the repeated click 2 response, showed that pharmacological treatments only had effects in the sham group. The cannabis extract increased the N40 click 2 response amplitude compared to nicotine (p = 2.7e-02) and cannabis extract + nicotine also increased the N40 click 2 amplitude compared to nicotine alone (p=6e-03; Figure 6A, bottom left). For noise-induced tinnitus mice the second click was unaltered by nicotine and/or cannabis extract (Figure 6A, bottom right). Examining the latency of the N40 response to the first click instead showed not alteration by either treatment in the sham group. For the noise-induced tinnitus group, cannabis extract + nicotine significantly delayed the click 1 N40 response compared to NaCl (p = 3.1e-02; Figure 6B, top right). For the repeated click 2 latency, the sham group instead showed decreased latency in the presence of cannabis extract compared to NaCl treatment (p = 1.4e-02; Figure 6B, bottom left). Again, the latency of the second click N40 response was not affected by nicotine and/or cannabis extract in noise-induced tinnitus mice (Figure 6B, bottom right). Next, examining the P80 amplitude and latency in detail only showed one effect on the second click latency for noise-induced tinnitus mice where cannabis extract + nicotine marginally increased the latency of P80 click 2 response compared to nicotine alone (p = 4.9e-02; Figure S4). All together we found the repeated second click N40 response to not be consistently modulated by treatment in noise-induced tinnitus mice, thereby agreeing with previous literature that pharmacological improvement of sensory gating affects the first click response (Amann et al., 2008; Rudnick et al., 2010).

Lastly we quantified the inter-peak interval (latency between the N40 and P80 peaks) of the response to the paired clicks (Figure S5). When double peaks were present, we measured latency from the first peak in the doublet (Figure S5A). We did not see any difference in the number of double N40 peaks recorded from sham and noise-induced tinnitus animals ($p > 0.07$ for all conditions tested; Figure S5B). Also, there were no significant differences in the inter-peak interval between negative and positive aERP for either treatments or groups ($F(1,20) < 2.06$, $p > 0.1$; Figure S5C). Thereby the average aERP waveform appears robust for latencies, despite individual variability. We confirmed our results by deriving the functional principal components from aERP data from a subset of animals where the pharmacologic treatment was found to affect the shape and smoothness specifically of the N40 component of auditory ERPs (effect size, $\eta^2 = 0.118$, $F(3,30) = 3.776$, p = 2.1e-02; Figure S6).

Taken together, this study found mice with noise-induced tinnitus to normally gate repetitive auditory stim-

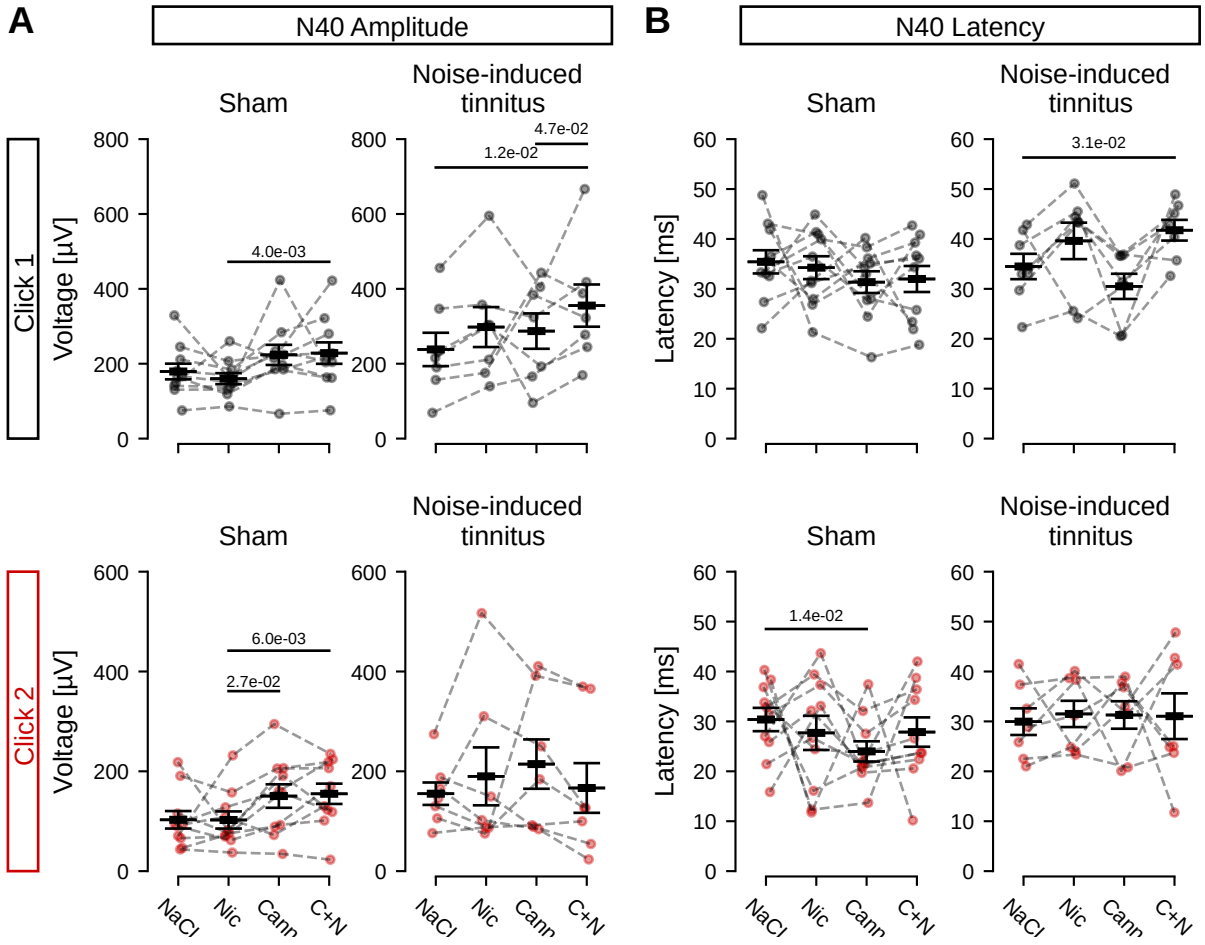

Figure 6: Noise-induced tinnitus mice only show modulation of the first click N40 response following cannabis+nicotine treatment. A) Comparison of the N40 amplitude in response to the first click (top) and second click (bottom) after saline, nicotine, cannabis extract and cannabis+nicotine administration for sham (left) and noise-induced tinnitus (right) mice. B) Latency comparisons between the first (top) and second (bottom) click responses in sham (left) and noise-induced tinnitus (right) animals across treatments. Only sham animals showed alterations of the second click amplitude and latency upon nicotine and cannabis treatment. Wilcoxon test, n = 10 sham and 7 noise-induced tinnitus mice.

uli, but showing larger amplitudes and slower processing of attention to repetitive clicks after pharmacological perturbations of the cholinergic and endocannabinoid systems, compared to sham-treated animals. The modulation of aERPs under nicotine and/or cannabis treatment was specifically related to the first click of the N40 component amplitude in noise-induced tinnitus mice.

Discussion

Using a mouse model of noise-induced tinnitus in absence of hearing threshold changes, we found that the N40 amplitude and latency is increased in animals with behavioral evidence of tinnitus. These mice showed increased ratio of the amplitude of first and second click N40 components upon cannabis and nicotine administration compared to sham animals, which indicates improvement in sensory gating. Cannabis administration also increased the latency ratio of the N40 component of aERPs for tinnitus compared to sham mice, indicating altered temporal processing. Our findings imply that the cholinergic and endocannabinoid systems are involved in perturbed sound processing in noise-induced tinnitus.

Tinnitus is a highly heterogeneous condition in humans (Cederroth et al., 2019), and the underlying pathophysiological mechanisms remain unclear. Recent evidence in animals and humans cumulate towards the involvement of the limbic system in tinnitus (Chen et al., 2015), however the confounding effects of hearing loss and hyperacusis make the disentangling of each contributing factor on the outcomes quite challenging (Khan et al., 2021). Here, we used a mouse model of noise-induced tinnitus in which hearing thresholds are kept at normal levels two days after noise-exposure, in order to avoid the confounding effect of hearing loss in temporal processing. To our knowledge, this is the first study to investigate sensory gating in the

hippocampus in mice with behavioral evidence of tinnitus and to evaluate how the cholinergic and endocannabinoid system interferes with sensory gating in these animals. A strength of this study is that hippocampal location for quantifying aERPs was standardized by anatomical post hoc examination and by electrophysiological profile (Scheffer-Teixeira et al., 2012) at each treatment session, thereby opening up for systematically testing a variety of compounds affecting limbic processing of attention to sound.

This study has several limitations. The assessment of tinnitus relied on GPIAS, which has been validated in rats against conditioning behavioral paradigms. In mice, such comparisons are lacking, and it remains unclear whether such measures truly reflect tinnitus. Previous studies conducted on CD-1 or CBA/CaJ mice exposed to noise, have revealed neural correlates for tinnitus in animals with impaired suppression of the startle by the gap (Li et al., 2013; Longenecker and Galazyuk, 2011), although these specific genetic backgrounds are not prone to an effective PPI or GPIAS (Yu et al., 2016) suggesting a very poor temporal processing in these strains. Evidence of reliable GPIAS after noise-induced tinnitus in C57BL/6J mice is to our knowledge missing. Yu et al. (2016) have shown reliable GPIAS in C57BL/6J at baseline and moderately impaired GPIAS after salicylate administration, suggestive of a mild tinnitus. Here, noise-induced tinnitus did not yield any specific tinnitus-like tone, rather it was spread over various frequencies. However, our ABR measures were limited to 16 kHz, due to speaker limitations, therefore hearing loss may have occurred at higher frequencies. We used a paradigm to select the most impacted frequency as a means to infer tinnitus in individual animals, however a proper validation of this approach is needed. Indeed, studies in animals and humans suggest that an increased ABR wave 5 latency is associated with tinnitus (Möhrle et al., 2019; Edvall et al., 2022). In spite of the lack of threshold changes after noise exposure, we found no evidence of such latency changes, nor lower Wave 1 amplitude as suggested in the literature as an indirect measure of synaptopathy (Kujawa and Liberman, 2009), potentially involved in tinnitus (Tziridis et al., 2021). It is thus possible that the tinnitus phenotype defined here is too mild to be correlated with alterations reminiscent of neural plasticity changes in the midbrain. Nonetheless, the hippocampal recordings performed here robustly detect alterations in animals with noise-induced tinnitus compared to sham, suggesting that the noise exposure had an incidence on temporal processing.

Another limitation is that the direct impact of nicotine and the cannabis extract on tinnitus were not assessed after the pharmacological intervention. Indeed, the connected headstage to collect ERP recordings did not allow animals to enter the restraining tube used to measure GPIAS. Previous studies have shown conflicting results (Zheng and Smith, 2019; Narwani et al., 2020). For instance, acute injection of the synthetic CB1/CB2 receptor agonists (WIN55,212-2, or CP55,940), exacerbate salicylate-induced tinnitus in rats assessed using a conditioned lick suppression paradigm (Zheng et al., 2010), whereas acute treatment with the CB1 receptor agonist arachidonyl-2-chloroethylamide (ACEA) had no effect (as measured by GPIAS) in guinea pigs with salicylate-induced tinnitus (Berger et al., 2017). It is possible that the confounding effects of stress on GPIAS measures caused by either salicylate or cannabis complexify the behavioral interpretation. Furthermore, cannabis extract concentration has shown U-shaped dose-response antidepressant effects in mice (El-Alfy et al., 2010), thereby evaluation of dose-dependent effects of activating the endocannabinoid system in different tinnitus models, as well as comparisons of administration routes of cannabis extract, is necessary in future studies.

Here we found that pharmacological manipulations of aERPs with both nicotine and cannabis extract improve sensory gating in noise-induced tinnitus mice but not in sham-treated animals. Our findings suggest that the higher N40 ratio under cannabis extract together with nicotine treatment in noise-induced tinnitus mice is related to an elevated click 1 amplitude and a lack of consistent modulation of the response to the second click, suggesting an increased registration (sensorial input processing) of the stimulus (Brockhaus-Dumke et al., 2008). Still, the cellular mechanisms underlying such alterations in sensory gating remain poorly understood.

In general, the endocannabinoid system dampens neuronal activity by activation of Gi-protein coupled presynaptic CB1 receptors that decrease neurotransmitter release through blocking of presynaptic voltage-gated calcium channels and opening of voltage-gated potassium (GIRK) channels, allowing potassium to flow out of the terminal (Kendall and Yudowski, 2016). For example, natural cannabis extracts can reduce neuronal hyperactivity in in vitro models of spasticity and epilepsy (Wilkinson et al., 2003) which is interesting since noise-induced tinnitus is related to neuronal hyperactivity of the auditory system (Shore et al., 2016). Still, the circuit effect of CB1 receptor activation depends on what type of presynaptic neuron expresses CB1 receptors (etc. glutamatergic or GABAergic cells) which can affect local plasticity differ-

ently (Kano, 2014). It is known that pyramidal cells of the hippocampus have relatively low expression of CB1 receptors (Kano et al., 2009) therefore we expect the cannabis extract to increase auditory input due to decreased inhibition, since CB1 receptors are strongly coexpressed with GAD65 in the hippocampus (Kano et al., 2009; Li et al., 2020), especially with strong CB1R expression on cholecystokinin positive interneurons (Li et al., 2020).

Furthermore this study use a THC-rich extract, which needs to be put in contrast to anxiolytic evaluation of THC at much lower doses (Kasten et al., 2019) and studies of seizure reduction by THC at doses as high as 100 mg/kg (Rosenberg et al., 2017). Still the concentration of THC in a cannabis extract cannot be compared to THC alone, but should be considered in relation to other cannabinoids present. For example, a systematic review of cannabinoid treatment of chronic pain found products with high-THC-to-CBD ratios the most useful for short-term relief of neuropathic chronic pain (McDonagh et al., 2022).

Here, we found the ability to suppress repetitive auditory stimuli to be preserved in noise-exposed mice, suggesting that noise-induced tinnitus without changes in hearing thresholds does not interfere with auditory gating; but that noise-induced tinnitus renders the response to auditory clicks abnormal in the presence of cannabis by delaying temporal coding. We also found that nicotine improves amplitude-ratio of aERPs in noise-exposed tinnitus mice, but in general, smoking is associated with greater risk of tinnitus (Biswas et al., 2022). Interestingly, human subjects administered orally a combination of a THC analog and nicotine have shown improved auditory deviant detection and mismatch negativity ERPs, but not when each drug was delivered alone (Salle et al., 2019). This interplay between the cholinergic and endocannabinoid system has been shown in basal forebrain cholinergic neurons expressing CB1Rs (Harkany et al., 2003). In detail, isolated cell studies showed decreased nicotinic currents generated by nicotinic $\alpha 7$ and $\alpha 4\beta 2$ subunit containing acetylcholine receptors in the presence of the endocannabinoid anandamide (Spivak et al., 2007). This could explain why the co-administration of nicotine and cannabis extract improves gating when compared to each isolated compound. Still, how the combination of nicotine and cannabis extract affects tinnitus patients needs to be better understood.

There has been an increased interest in studying the endocannabinoid system in animals models of tinnitus (Berger et al., 2017; Narwani et al., 2020). Due to the availability of a transgenic line targeting Cre expression at cells expressing the alpha-2 nicotinic receptor (Leao et al., 2012), the role of the cholinergic system in tinnitus could be investigated by using chemogenetics to locally manipulate the excitability of these cells during aERP recordings; or in tinnitus induction performing similar manipulations during noise exposure. A similar approach would be difficult for investigating the role of the endocannabinoid system in tinnitus due to the unavailability of specific targeting of, for example, CB1-expressing cells. However, the depletion of GLAST to exacerbate the tinnitus phenotype, may also be more appropriate to investigate in greater details the underlying cellular and molecular mechanisms (Yu et al., 2016). Still, it is becoming clear that loud noise activates both auditory and limbic pathways (Zhang et al., 2018) but how prolonged noise-exposure alters sound processing of each system needs to be further examined, as well as how the limbic and auditory systems interact in tinnitus (Qu et al., 2019).

In conclusion, our study shows that provoking auditory event-related potentials pharmacologically, using nicotine and/or cannabis extract rich in THC, showed noise-induced tinnitus mice to improve gating of the N40 component especially under the combined influence of cannabis extract and nicotine, by increasing the first click response amplitude. However, cannabis extract also increased the latency ratio of the N40 component in noise-induced tinnitus mice compared to sham animals, indicating delayed temporal processing of paired clicks. Thereby the activation of the cholinergic and endocannabinoid system have distinct and different effects on auditory gating in the context of tinnitus.

Conflict of Interest Statement

The authors declare that the research was conducted in the absence of any commercial or financial relationships that could be construed as a potential conflict of interest.

Author Contributions

KEL and BC designed the study. BC and TM performed experiments; SRBS analyzed the cannabis extract; BC, TM and TZL analyzed the data; BC, CRC and KEL wrote the manuscript with important input from TM and TZL.

Funding

This work is supported by the American Tinnitus Association and the Brazilian funding agency CAPES - Coordenação de Aperfeiçoamento de Pessoal de Nível Superior. CRC is supported by the GENDER-Net Co-Plus Fund (GNP-182), the European Union's Horizon 2020 Research and Innovation Programme, Grant Agreement No 848261 and the European Union's Horizon 2020 research and innovation programme under the Marie Skłodowska-Curie grant agreement No 722046. TM is supported by the Wenner-Gren Stiftelserna (UPD2020-0006 and UPD2021-0114).

Acknowledgments

The authors thank Dr Cláudio Queiroz at the Brain Institute-UFRN for providing the cannabis extract and Dr Jessica Winne for technical assistance in electrode manufacturing.

Data Availability Statement

The datasets generated and/or analyzed in the current study are available on request. Recordings were done using the Open-ephys GUI (Siegle et al., 2015). Stimulation and data analysis were performed using SciScripts (Malfatti, 2022), Scipy (Virtanen et al., 2020) and Numpy (Harris et al., 2020). Statistical analysis used for functional data analysis (Figure S6) was carried out with R software (R Core Team, 2020) and the functional data analysis package (Ramsay et al., 2009). All plots were produced using Matplotlib (Hunter, 2007), and schematics were done using Inkscape (Inkscape Project, 2022). All scripts used for recordings and analysis are available online (Ciralli et al., 2022).

References

Amann, L. C., Phillips, J. M., Halene, T. B., and Siegel, S. J. (2008). Male and female mice differ for baseline and nicotine-induced event related potentials. *Behavioral neuroscience* 122, 982

Asokan, M., Williamson, R., Hancock, K., and Polley, D. (2018). Sensory overamplification in layer 5 auditory corticofugal projection neurons following cochlear nerve synaptic damage. *Nat. Commun* 9, 2468. doi:10.1038/s41467-018-04852-y.

Ballinger, E., Ananth, M., Talmage, D., and Role, L. (2016). Basal forebrain cholinergic circuits and signaling in cognition and cognitive decline. *Neuron* 91, 1199–1218. doi:10.1016/j.neuron.2016.09.006.

Berger, J. I., Coomber, B., Hill, S., Alexander, S. P., Owen, W., Palmer, A. R., et al. (2017). Effects of the cannabinoid cb1 agonist acea on salicylate ototoxicity, hyperacusis and tinnitus in guinea pigs. *Hearing research* 356, 51–62

Biswas, R., Lugo, A., Akeroyd, M. A., Schlee, W., Gallus, S., and Hall, D. (2022). Tinnitus prevalence in europe: a multi-country cross-sectional population study. *The Lancet Regional Health-Europe* 12, 100250

Böcker, K., Gerritsen, J., Hunault, C., Kruidenier, M., Mensinga, T. T., and Kenemans, J. (2010). Cannabis with high Δ9-thc contents affects perception and visual selective attention acutely: an event-related potential study. *Pharmacology Biochemistry and Behavior* 96, 67–74

Brockhaus-Dumke, A., Mueller, R., Faigle, U., and Klosterkoetter, J. (2008). Sensory gating revisited: relation between brain oscillations and auditory evoked potentials in schizophrenia. *Schizophr. Res* 99, 238–249. doi:10.1016/j.schres.2007.10.034.

Campbell, J., Bean, C., and LaBrec, A. (2018). Normal hearing young adults with mild tinnitus: Reduced inhibition as measured through sensory gating. *Audiology research* 8

Cederroth, C. R., PirouziFard, M., Trpchevska, N., Idrizbegovic, E., Canlon, B., Sundquist, J., et al. (2019). Association of genetic vs environmental factors in swedish adoptees with clinically significant tinnitus. *JAMA Otolaryngology–Head & Neck Surgery* 145, 222. doi:10.1001/jamaoto.2018.3852

Chen, Y.-C., Li, X., Liu, L., Wang, J., Lu, C.-Q., Yang, M., et al. (2015). Tinnitus and hyperacusis involve hyperactivity and enhanced connectivity in auditory-limbic-arousal-cerebellar network. *elife* 4, e06576. doi:10.7554/elife.06576.001

Cima, R., Mazurek, B., Haider, H., Kikidis, D., Lapira, A., and Noreña, A. (2019). A multidisciplinary european guideline for tinnitus: diagnostics, assessment, and treatment. *HNO* 67, 10–42. doi:10.1007/s00106-019-0633-7.

[Dataset] Ciralli, B., Malfatti, T., and Lima, T. Z. (2022). Sensorygatingontinnitus2022. doi:10.5281/ZENODO.6645914

Connolly, P., Maxwell, C., Liang, Y., Kahn, J., Kanes, S., and Abel, T. (2004). The effects of ketamine vary among inbred mouse strains and mimic schizophrenia for the p80, but not p20 or n40 auditory erp components. *Neurochem. Res* 29, 1179–1188

Edvall, N., Mehraei, G., Claeson, M., Lazar, A., Bulla, J., and Leineweber, C. (2022). Alterations in auditory brainstem response distinguish occasional and constant tinnitus. *J. Clin. Invest* doi:10.1172/JCI155094.

El-Alfy, A. T., Ivey, K., Robinson, K., Ahmed, S., Radwan, M., Slade, D., et al. (2010). Antidepressant-like effect of δ9-tetrahydrocannabinol and other cannabinoids isolated from cannabis sativa l. *Pharmacology Biochemistry and Behavior* 95, 434–442. doi:10.1016/j.pbb.2010.03.004

Harkany, T., Härtig, W., Berghuis, P., Dobszay, M., Zilberter, Y., and Edwards, R. (2003). Complementary distribution of type 1 cannabinoid receptors and vesicular glutamate transporter 3 in basal forebrain suggests input-specific retrograde signalling by cholinergic neurons. *Eur. J. Neurosci* 18, 1979–1992. doi:10.1046/j.1460-9568.2003.02898.x.

Harris, C. R., Millman, K. J., van der Walt, S. J., Gommers, R., Virtanen, P., Cournapeau, D., et al. (2020). Array programming with NumPy. *Nature* 585, 357–362. doi:10.1038/s41586-020-2649-2

Henry, K. (1979). Auditory brainstem volume-conducted responses: origins in the laboratory mouse. *J. Am. Aud. Soc* 4, 173–178

Hiller, W. and Goebel, G. (2006). Factors influencing tinnitus loudness and annoyance. *Arch. Otolaryngol. Head Neck Surg* 132, 1323–1330. doi:10.1001/archotol.132.12.1323.

Hunter, J. D. (2007). Matplotlib: A 2d Graphics Environment. *Computing in Science & Engineering* 9, 90–95. doi:10.1109/MCSE.2007.55

[Dataset] Inkscape Project (2022). Inkscape

Johansson, E., Ohlsson, A., Lindgren, J.-E., Agurell, S., Gillespie, H., and Hollister, L. E. (1987). Single-dose kinetics of deuterium-labelled cannabinol in man after intravenous administration and smoking. *Biological Mass Spectrometry* 14, 495–499. doi:10.1002/bms.1200140904

Kano, M. (2014). Control of synaptic function by endocannabinoid-mediated retrograde signaling. *Proc. Jpn. Acad. Ser. B Phys. Biol. Sci* 90, 235–250

Kano, M., Ohno-Shosaku, T., Hashimotodani, Y., Uchigashima, M., and Watanabe, M. (2009). Endocannabinoid-mediated control of synaptic transmission. *Physiol. Rev* 89, 309–380. doi:10.1152/physrev.00019.2008.

Kasten, C., Zhang, Y., and Boehm, S. (2019). Acute cannabinoids produce robust anxiety-like and locomotor effects in mice, but long-term consequences are age- and sex-dependent. *Front. Behav. Neurosci* 13, 32. doi:10.3389/fnbeh.2019.00032.

Kendall, D. and Yudowski, G. (2016). Cannabinoid receptors in the central nervous system: Their signaling and roles in disease. *Front. Cell. Neurosci* 10, 294. doi:10.3389/fncel.2016.00294.

Khan, R. A., Sutton, B. P., Tai, Y., Schmidt, S. A., Shahsavarani, S., and Husain, F. T. (2021). A large-scale diffusion imaging study of tinnitus and hearing loss. *Scientific Reports* 11. doi:10.1038/s41598-021-02908-6

Kujawa, S. G. and Liberman, M. C. (2009). Adding insult to injury: Cochlear nerve degeneration after "temporary" noise-induced hearing loss. *Journal of Neuroscience* 29, 14077–14085. doi:10.1523/jneurosci.2845-09.2009

Langguth, B., Landgrebe, M., Kleinjung, T., Sand, G., and Hajak, G. (2011). Tinnitus and depression. *World J. Biol. Psychiatry Off. J. World Fed. Soc. Biol. Psychiatry* 12, 489–500. doi:10.3109/15622975.2011.575178.

Lanting, C., Kleine, E., and Dijk, P. (2009). Neural activity underlying tinnitus generation: results from pet and fmri. *Hear. Res* 255, 1–13. doi:10.1016/j.heares.2009.06.009.

Leao, R., Mikulovic, S., Leao, K., Munguba, H., Gezelius, H., and Enjin, A. (2012). Olm interneurons differentially modulate ca3 and entorhinal inputs to hippocampal ca1 neurons. *Nat. Neurosci* 15, 1524–1530. doi:10.1038/nn.3235.

Li, H., Yang, J., Tian, C., Diao, M., Wang, Q., and Zhao, S. (2020). Organized cannabinoid receptor distribution in neurons revealed by super-resolution fluorescence imaging. *Nat. Commun* 11, 5699. doi:10.1038/s41467-020-19510-5.

Li, S., Choi, V., and Tzounopoulos, T. (2013). Pathogenic plasticity of kv7.2/3 channel activity is essential for the induction of tinnitus. *Proc. Natl. Acad. Sci. U. S. A* 110, 9980–9985. doi:10.1073/pnas.1302770110.

Lijffijt, M., Lane, S., Meier, S., Boutros, N., Burroughs, S., and Steinberg, J. (2009). P50, n100, and p200 sensory gating: Relationships with behavioral inhibition, attention, and working memory. *Psychophysiology* 46, 1059. doi:10.1111/j.1469-8986.2009.00845.x.

Longenecker, R. and Galazyuk, A. (2016). Variable effects of acoustic trauma on behavioral and neural correlates of tinnitus in individual animals. *Front. Behav. Neurosci* 10, 207. doi:10.3389/fnbeh.2016.00207.

Longenecker, R. J. and Galazyuk, A. V. (2011). Development of tinnitus in CBA/CaJ mice following sound exposure. *Journal of the Association for Research in Otolaryngology* 12, 647–658. doi:10.1007/s10162-011-0276-1

[Dataset] Malfatti, T. (2022). Sciscripts. doi:10.5281/ZENODO.4045872

Malfatti, T., Ciralli, B., Hilscher, M. M., Leao, R. N., and Leao, K. E. (2022). Decreasing dorsal cochlear nucleus activity ameliorates noise-induced tinnitus perception in mice. *BMC Biology* 20. doi:10.1186/s12915-022-01288-1

McDonagh, M. S., Morasco, B. J., Wagner, J., Ahmed, A. Y., Fu, R., Kansagara, D., et al. (2022). Cannabis-based products for chronic pain: A systematic review. *Annals of Internal Medicine* doi:https://doi.org/10.7326/M21-4520

Metzger, K. L., Maxwell, C. R., Liang, Y., and Siegel, S. J. (2007). Effects of nicotine vary across two auditory evoked potentials in the mouse. *Biological psychiatry* 61, 23–30

Möhrle, D., Hofmeier, B., Amend, M., Wolpert, S., Ni, K., Bing, D., et al. (2019). Enhanced central neural gain compensates acoustic trauma-induced cochlear impairment, but unlikely correlates with tinnitus and hyperacusis. *Neuroscience* 407, 146–169. doi:10.1016/j.neuroscience.2018.12.038

Narwani, V., Bourdillon, A., Nalamada, K., Manes, R., and Hildrew, D. (2020). Does cannabis alleviate tinnitus? a review of the current literature. *Laryngoscope Investig. Otolaryngol* 5, 1147–1155. doi:10.1002/lio2.479.

Petersen, D., Norris, K., and Thompson, J. (1984). A comparative study of the disposition of nicotine and its metabolites in three inbred strains of mice. *Drug Metabolism and Disposition* 12, 725–731

Qu, T., Qi, Y., Yu, S., Du, Z., Wei, W., and Cai, A. (2019). Dynamic changes of functional neuronal activities between the auditory pathway and limbic systems contribute to noise-induced tinnitus with a normal audiogram. *Neuroscience* 408, 31–45. doi:10.1016/j.neuroscience.2019.03.054.

[Dataset] R Core Team (2020). R: A language and environment for statistical computing

Ramsay, J., Hooker, G., and Graves, S. (2009). Introduction to functional data analysis. In *Functional Data Analysis with R and MATLAB Use R*, eds. J. Ramsay, G. Hooker, and S. Graves (New York, NY: Springer). 1–19. doi:10.1007/978-0-387-98185-7_1.

Rosenberg, E. C., Patra, P. H., and Whalley, B. J. (2017). Therapeutic effects of cannabinoids in animal models of seizures, epilepsy, epileptogenesis, and epilepsy-related neuroprotection. *Epilepsy and Behavior* 70, 319–327. doi:10.1016/j.yebeh.2016.11.006

Rudnick, N., Strasser, A., Phillips, J., Jepson, C., Patterson, F., and Frey, J. (2010). Mouse model predicts effects of smoking and varenicline on event-related potentials in humans. *Nicotine Tob. Res. Off. J. Soc. Res. Nicotine Tob* 12, 589–597. doi:10.1093/ntr/ntq049.

Salle, S., Inyang, L., Impey, D., Smith, D., Choueiry, J., and Nelson, R. (2019). Acute separate and combined effects of cannabinoid and nicotinic receptor agonists on mmn-indexed auditory deviance detection in healthy humans. *Pharmacol. Biochem. Behav* 184, 172739. doi:10.1016/j.pbb.2019.172739.

Sampson, P. B. (2020). Phytocannabinoid pharmacology: Medicinal properties of cannabis sativa constituents aside from the big two. *Journal of Natural Products* 84, 142–160. doi:10.1021/acs.jnatprod.0c00965

Santos Filha, V. and Matas, C. (2010). Late auditory evoked potentials in individuals with tinnitus. *Braz. J. Otorhinolaryngol* 76, 263–270

Scheffer-Teixeira, R., Belchior, H., Caixeta, F., Souza, B., Ribeiro, S., and Tort, A. (2012). Theta phase modulates multiple layer-specific oscillations in the ca1 region. *Cereb. Cortex N. Y. N* 22, 2404–2414. doi:10.1093/cercor/bhr319.

Shore, S., Roberts, L., and Langguth, B. (2016). Maladaptive plasticity in tinnitus–triggers, mechanisms and treatment. *Nat. Rev. Neurol* 12, 150–160. doi:10.1038/nrneurol.2016.12.

Siegle, J. H., Hale, G. J., Newman, J. P., and Voigts, J. (2015). Neural ensemble communities: open-source approaches to hardware for large-scale electrophysiology. *Current Opinion in Neurobiology* 32, 53–59. doi:10.1016/j.conb.2014.11.004

Spivak, C., Lupica, C., and Oz, M. (2007). The endocannabinoid anandamide inhibits the function of alpha4beta2 nicotinic acetylcholine receptors. *Mol. Pharmacol* 72, 1024–1032. doi:10.1124/mol.107.036939.

Sturm, J., Zhang-Hooks, Y.-X., Roos, H., Nguyen, T., and Kandler, K. (2017). Noise trauma-induced behavioral gap detection deficits correlate with reorganization of excitatory and inhibitory local circuits in the inferior colliculus and are prevented by acoustic enrichment. *J. Neurosci. Off. J. Soc. Neurosci* 37, 6314–6330. doi:10.1523/JNEUROSCI.0602-17.2017.

Tai, Y. and Husain, F. T. (2019). The role of cognitive control in tinnitus and its relation to speech-in-noise performance. *Journal of audiology & otology* 23, 1

Torrens, A., Vozella, V., Huff, H., McNeil, B., Ahmed, F., and Ghidini, A. (2020). Comparative pharmacokinetics of Δ9-tetrahydrocannabinol in adolescent and adult male mice. *J. Pharmacol. Exp. Ther* 374, 151–160. doi:10.1124/jpet.120.265892.

Turner, J., Brozoski, T., Bauer, C., Parrish, J., Myers, K., and Hughes, L. (2006). Gap detection deficits in rats with tinnitus: a potential novel screening tool. *Behav. Neurosci* 120, 188–195. doi:10.1037/0735-7044.120.1.188.

Tziridis, K., Forster, J., Buchheidt-DÃ¶rfler, I., Krauss, P., Schilling, A., Wendler, O., et al. (2021). Tinnitus development is associated with synaptopathy of inner hair cells in mongolian gerbils. *European Journal of Neuroscience* 54, 4768–4780. doi:10.1111/ejn.15334

Verrico, C., Jentsch, J., Roth, R., and Taylor, J. (2004). Repeated, intermittent delta(9)-tetrahydrocannabinol administration to rats impairs acquisition and performance of a test of visuospatial divided attention. *Neuropsychopharmacol. Off. Publ. Am. Coll. Neuropsychopharmacol* 29, 522–529. doi:10.1038/sj.npp.1300316.

Virtanen, P., Gommers, R., Oliphant, T. E., Haberland, M., Reddy, T., Cournapeau, D., et al. (2020). SciPy 1.0: Fundamental Algorithms for Scientific Computing in Python. *Nature Methods* 17, 261–272. doi:10.1038/s41592-019-0686-2

Wilkinson, J., Whalley, B., Baker, D., Pryce, G., Constanti, A., and Gibbons, S. (2003). Medicinal cannabis: is Δ9–tetrahydrocannabinol necessary for all its effects? *J. Pharm. Pharmacol* 55, 1687–1694. doi:10.1211/0022357022304.

Xu, C., Chang, T., Du, Y., Yu, C., Tan, X., and Li, X. (2019). Pharmacokinetics of oral and intravenous cannabidiol and its antidepressant-like effects in chronic mild stress mouse model. *Environmental Toxicology and Pharmacology* 70, 103202. doi:10.1016/j.etap.2019.103202

Yu, H., Vikhe Patil, K., Han, C., Fabella, B., Canlon, B., and Someya, S. (2016). Glast deficiency in mice exacerbates gap detection deficits in a model of salicylate-induced tinnitus. *Front. Behav. Neurosci* 10, 158. doi:10.3389/fnbeh.2016.00158.

Zeng, F., Richardson, M., and Turner, K. (2020). Tinnitus does not interfere with auditory and speech perception. *J. Neurosci* doi:10.1523/JNEUROSCI.0396-20.2020.

Zhang, G.-W., Sun, W.-J., Zingg, B., Shen, L., He, J., Xiong, Y., et al. (2018). A non-canonical reticular-limbic central auditory pathway via medial septum contributes to fear conditioning. *Neuron* 97, 406–417.e4. doi:10.1016/j.neuron.2017.12.010

Zhang, W., Peng, Z., Yu, S., Song, Q.-L., Qu, T.-F., Liu, K., et al. (2020). Exposure to sodium salicylate disrupts VGLUT3 expression in cochlear inner hair cells and contributes to tinnitus. *Physiological Research* , 181–190doi:10.33549/physiolres.934180

Zheng, Y. and Smith, P. (2019). Cannabinoid drugs: will they relieve or exacerbate tinnitus? curr. *Opin. Neurol* 32, 131–136. doi:10.1097/WCO.0000000000000631.

Zheng, Y., Stiles, L., Hamilton, E., Smith, P., and Darlington, C. (2010). The effects of the synthetic cannabinoid receptor agonists, win55,212-2 and cp55,940, on salicylate-induced tinnitus in rats. *Hear. Res* 268, 145–150. doi:10.1016/j.heares.2010.05.015.